Inorg. Chem. **2008**, *47*, 5324−5331

From Unstable to Stable: Half-Metallocene Catalysts for Olefin Polymerization†

Prabhuodeyara M. Gurubasavaraj, Herbert W. Roesky,* Bijan Nekoueishahraki, Aritra Pal, and Regine Herbst-Irmer

Institute of Inorganic Chemistry, University of Göttingen, Tammannstrasse 4, 37077 Göttingen, Germany

Received January 31, 2008

The reaction of LAlMeOH [L = CH(N(Ar)(CMe))$_2$, Ar = 2,6-*i*-Pr$_2$C$_6$H$_3$] with CpTiMe$_3$, Cp*TiMe$_3$, and Cp*ZrMe$_3$ was investigated to yield LAlMe(μ-O)TiMe$_2$Cp (**2**), LAlMe(μ-O)TiMe$_2$Cp* (**3**), and LAlMe(μ-O)ZrMe$_2$Cp* (**4**), respectively. The resulting compounds **2**−**4** are stable at elevated temperatures, in contrast to their precursors such as CpTiMe$_3$ and Cp*ZrMe$_3$, which already decompose below room temperature. Compounds **2**−**4** were characterized by single-crystal X-ray structural analysis. Compounds **2** and **3** were tested for ethylene polymerization in the presence of methylaluminoxane. The half-metallocene complex **3** has higher activity compared to **2**. The polydispersities are in the range from 2.8 to 4.2. A copolymerization with styrene was not observed.

Introduction

Well-defined "single-site" metallocene catalysts have been attracting immense research interest over conventional Ziegler−Natta heterogeneous catalysts.[1] This is mainly due to the fact that metallocene catalysts in combination with methylaluminoxane (MAO) exhibit higher stereoselectivity, narrower molecular weight distribution, and high catalytic activity in ethylene, propylene, and styrene polymerization.[1,2] Other advantages are that these systems produce structurally well-defined "single-site" active catalytic species.[3] This leads to a variety of high-performance polyolefin products including isotactic,[2] syndiotactic,[4] and atactic polypropylenes,[5] high-density polyethylene (PE),[6] linear low-density PE,[7] syndiotactic polystyrene (PS),[8] and cycloolefin copolymers[9] with a uniform and tuneable microstructure.

In spite of the success of metallocene catalysts in polymerization reactions, they also exhibit some disadvantages. These catalysts need a large amount of MAO or expensive fluorinated borate activators to obtain adequate polymerization activity, which causes concern over the high cost of metallocene catalysts and the high ash content (Al_2O_3) of the product polymers. Consequently, there is a great need to develop new catalyst systems that can provide high catalytic activity with no need for a large amount of expensive cocatalysts. The design and synthesis of new transition-metal catalyst precursors and main-group organometallic cocatalysts is a very important subject that can provide high catalytic activity with low cocatalyst-to-catalyst precursor ratios and allows unprecedented control over the polymer microstructure, producing new polymers with improved polymer properties. The growing demand for high-performance polymer products has inspired extensive academic and industrial research interest in developing new efficient catalysts that can produce polymers of significant rheological and mechanical properties.

The development of these metallocene catalysts was closely related to the discovery of MAO as a cocatalyst, which is thought to generate a cationic metal alkyl active

† Dedicated to Professor George M. Sheldrick on the occasion of his 65th birthday.

* To whom correspondence should be addressed. E-mail: hroesky@gwdg.de.

(1) Kaminsky, W.; Külper, K.; Brintzinger, H. H.; Wild, F. R. W. P. *Angew. Chem.* **1985**, *97*, 507–508; *Angew. Chem., Int. Ed. Engl.* **1985**, *24*, 507−508.
(2) Ewen, J. A. *J. Am. Chem. Soc.* **1984**, *106*, 6355–6364.
(3) Chen, E. Y.-X.; Marks, T. J. *Chem. Rev.* **2000**, *100*, 1391–1434, and references cited therein.
(4) Alt, H. G.; Samuel, E. *Chem. Soc. Rev.* **1998**, *27*, 323–329.
(5) Enders, M.; Fernandez, P.; Ludwig, G.; Pritzkow, H. *Organometallics* **2001**, *20*, 5005–5007.
(6) Piel, C.; Stadler, F. J.; Kaschta, J.; Rulhoff, S.; Münstedt, H.; Kaminsky, W. *Macromol. Chem. Phys.* **2006**, *207*, 26–38.
(7) Bae, C.; Hartwig, J. F.; Chung, H.; Harris, N. K.; Switek, K. A.; Hillmyer, M. A. *Angew. Chem.* **2005**, *117*, 6568–6571; *Angew. Chem., Int. Ed.* **2005**, *44*, 6410−6413.
(8) Kaminsky, W.; Lenk, S.; Scholz, V.; Roesky, H. W.; Herzog, A. *Macromolecules* **1997**, *30*, 7647–7650.
(9) Kaminsky, W.; Arndt, M. *Metallocene-Based Polyolefins*; Scheirs, J., Kaminsky, W., Eds.; Wiley: New York, 2000; p 91.

10.1021/ic800198e CCC: $40.75
Published on Web 05/21/2008

site by alkylation of the catalyst precursor and abstraction of anionic substituents.[3] Recently, we isolated the unprecedented LAlMeOH [**1**; L = CH(N(Ar)(CMe))$_2$, Ar = 2,6-*i*-Pr$_2$C$_6$H$_3$], which has only one −[AlMeO]− unit, and its reaction with group 4 metallocene compounds for the design of well-defined highly active homogeneous catalysts that exhibit high catalytic activity in olefin polymerization.[10] The oxophilicity of group 4 metals and Brönsted acidic character of the Al(O−H) moiety resulted in the isolation of complexes containing the Al(μ-O)M (M = Ti, Zr, Hf) fragment, which is known to exhibit high activity in olefin polymerization.[10,11]

The formation and stability of the cation is one of the key steps in the polymerization reaction. It depends on the electronic and steric bulk of the ligand that surrounds the metal center. The stability of the cation leads to the "living catalyst" character, which increases the catalytic activity in the polymerization reaction and produces narrowly distributed high molecular weight polymers.[12]

Recently, we studied the role of oxygen in homogeneous heterobimetallic complexes of zirconium and titanium. Theoretical studies on the complexes reveal that the oxygen enhances the intrinsic Lewis acidity at the metal centers, which, as a consequence, requires a lower amount of MAO to produce "cation-like" highly electrophilic active species, which catalyze the polymerization reaction.[13]

Although considerable attention has been devoted to the synthesis, characterization, and catalytic studies of sandwich metallocene complexes,[14,15] homogeneous half-metallocene complexes of group 4 metals bearing terminal methyl groups (except for Cp*TiMe$_3$) have received little attention because of the instability of these complexes at ambient temperature.[16] However, in recent decades, there is growing interest[17,18] in monocyclopentadienyl group 4 metal complexes because of the fact that the most active catalysts are those containing the lowest number of valence electrons.[19] The recent developments of monocyclopentadienyl-based metallocene catalysts are heterogeneous oxide-supported complexes of the type Cp*MMe$_3$ (M = Ti, Zr) for olefin polymerization. These systems exhibit moderate-to-good catalytic activity and were characterized by some advanced techniques (such as ^{13}C CPMAS and EXAFS).[20] There are some reports on zirconium and titanium compounds bearing bulky Cp* ligands and terminal methyl groups.[21] However, preparation of the complexes bearing one Cp and methyl groups on the metal centers still remains a synthetic challenge. Overall, well-characterized and catalytically well-studied compounds with one Cp and methyl substituents are still elusive.

In this contribution, we report a facile route for the preparation and catalytic property of Al(μ-O)M (M = Ti, Zr) containing half-metallocene (Cp′ = C$_5$H$_5$ or C$_5$Me$_5$) complexes by a tailor-made precursor such as **1**. The monocyclopentadienyl metallocene complexes attached to the LMeAlO fragment were structurally characterized and used for the olefin polymerization and copolymerization of styrene and ethylene. These complexes exhibit high activity toward olefin polymerization and produce linear PE.

(10) Bai, G.; Singh, S.; Roesky, H. W.; Noltemeyer, M.; Schmidt, H.-G. *J. Am. Chem. Soc.* **2005**, *127*, 3449–3455.

(11) Gurubasavaraj, P. M.; Mandal, S. K.; Roesky, H. W.; Oswald, R. B.; Pal, A.; Noltemeyer, M. *Inorg. Chem.* **2007**, *46*, 1056–1061.

(12) Manivannan, R.; Sundarajan, G. *Macromolecules* **2002**, *35*, 7883–7890.

(13) Gurubasavaraj, P. M.; Roesky, H. W.; Sharma, P. M. V.; Oswald, R. B.; Dolle, V.; Herbst-Irmer, R.; Pal, A. *Organometallics* **2007**, *26*, 3346–3351.

(14) For example, see; (a) Erker, G.; Kehr, G.; Fröhlich, R. *Coord. Chem. Rev.* **2006**, *250*, 36–46. (b) Erker, G.; Kehr, G.; Fröhlich, R. *J. Organomet. Chem.* **2004**, *689*, 1402–1412. (c) Collins, S.; Ward, D. G. *J. Am. Chem. Soc.* **1992**, *114*, 5460–5462. (d) Williams, V. C.; Dai, C.; Li, Z.; Collins, S.; Piers, W. E.; Clegg, W.; Elsegood, M. R. J.; Marder, T. B. *Angew. Chem.* **1999**, *111*, 3922–3926; *Angew. Chem., Int. Ed.* **1999**, *38*, 3695−3698. (e) Stojcevic, G.; Kim, H.; Taylor, N. J.; Marder, T. B.; Collins, S. *Angew. Chem.* **2004**, *116*, 5639–5642; *Angew. Chem., Int. Ed.* **2004**, *43*, 5523−5526. (f) Kotov, V. V.; Fröhlich, R.; Kehr, G.; Erker, G. *J. Organomet. Chem.* **2003**, *676*, 1–7. (g) Miyazawa, A.; Kase, T.; Hashimoto, K.; Choi, J.-c.; Sakakura, T.; Ji-zhu, J. *Macromolecules* **2004**, *37*, 8840–8845. (h) Mahanthappa, M. K.; Cole, A. P.; Waymouth, R. M. *Organometallics* **2004**, *23*, 836–845. (i) Nomura, K.; Fujii, K. *Macromolecules* **2003**, *36*, 2633–2641. (j) Nomura, K.; Okumura, H.; Komatsu, T.; Naga, N. *Macromolecules* **2002**, *35*, 5388–5395. (k) Chirik, P. J.; Bercaw, J. E. *Organometallics* **2005**, *24*, 5407–5423. (l) Joung, U. G.; Lee, B. Y. *Polyhedron* **2005**, *24*, 1256–1261.

(15) For example, see: (a) Arndt, P.; Spannenberg, A.; Baumann, W; Becke, S.; Rosenthal, U. *Eur. J. Inorg. Chem.* **2001**, 2885–2890. (b) Andrés, R.; de Jesus, E.; de la Mata, F. J.; Flores, J. C.; Gómez, R. *Eur. J. Inorg. Chem.* **2002**, 2281–2286. (c) Coates, G. W. *Chem. Rev.* **2000**, *100*, 1223–1252. (d) Bochmann, M. *J. Chem. Soc., Dalton Trans.* **1996**, 255–270. (e) Alt, H. G.; Köppl, A. *Chem. Rev.* **2000**, *100*, 1205–1221. (f) Kaminsky, W. *J. Chem. Soc., Dalton Trans.* **1998**, 1413–1418. (g) Resconi, L.; Cavallo, L.; Fait, A.; Piemontesi, F. *Chem. Rev.* **2000**, *100*, 1253–1345. (h) Erker, G. *Acc. Chem. Res.* **2001**, *34*, 309–317. (i) Erker, G. *Acc. Chem. Res.* **1984**, *17*, 103–109. (j) Rappé, A. K.; Skiff, W. M.; Casewit, C. J. *Chem. Rev.* **2000**, *100*, 1435–1456. (k) Boffa, L. S.; Novak, B. M. *Chem. Rev.* **2000**, *100*, 1479–1493. (l) Arndt, P.; Burlakov, V. V.; Spannenberg, A.; Rosenthal, U. *Inorg. Chem. Commun.* **2007**, *10*, 792–794. (m) Rosenthal, U.; Burlakov, V. V.; Bach, M. A.; Beweries, T. *Chem. Soc. Rev.* **2007**, *36*, 719–728, and references cited therein.

(16) (a) Giannini, U.; Cesca, S. *Tetrahedron Lett.* **1960**, *1*, 19–20. (b) Mena, M.; Royo, P.; Serrano, R.; Pellinghelli, M. A.; Tiripicchio, A. *Organometallics* **1989**, *8*, 476–482. (c) Wolczanski, P. T.; Bercaw, J. E. *Organometallics* **1982**, *1*, 793–799.

(17) For example, see: (a) Nomura, K.; Naga, N.; Miki, M.; Yanagi, K.; Imai, A. *Organometallics* **1998**, *17*, 2152–2154. (b) Nomura, K.; Hatanaka, Y.; Okumura, H.; Fujiki, M.; Hasegawa, K. *Macromolecules* **2004**, *37*, 1693–1695. (c) Wang, W.; Fujiki, M.; Nomura, K. *J. Am. Chem. Soc.* **2005**, *127*, 4582–4583. (d) Nomura, K.; Takemoto, A.; Hatanaka, Y.; Okumura, H.; Fujiki, M.; Hasegawa, K. *Macromolecules* **2006**, *39*, 4009–4017. (e) Kitiyanan, B.; Nomura, K. *Organometallics* **2007**, *26*, 3461–3465. (f) Erben, M.; Merna, J.; Hermanová, S.; Cisarová, I.; Padelková, Z.; Dusek, M. *Organometallics* **2007**, *26*, 2735–2741.

(18) For example, see: (a) Poli, R. *Chem. Rev.* **1991**, *91*, 509–551. (b) Baird, M. C. *Chem. Rev.* **2000**, *100*, 1471–1478. (c) Phomphrai, K.; Fenwick, A. E.; Sharma, S.; Fanwick, P. E.; Caruthers, J. M.; Delgass, W. N.; Abu-Omar, M. M.; Rothwell, I. P. *Organometallics* **2006**, *25*, 214–220. (d) Cheng, X.; Slebodnick, C.; Deck, P. A.; Billodeaux, D. R.; Fronczek, F. R. *Inorg. Chem.* **2000**, *39*, 4921–4926. (e) Noh, S. K.; Jung, W.; Oh, H.; Lee, Y. R.; Lyoo, W. S. *J. Organomet. Chem.* **2006**, *691*, 5000–5006. (f) Ramos, C.; Royo, P.; Lanfranchi, M.; Pellinghelli, M. A.; Tiripicchio, A. *Organometallics* **2007**, *26*, 445–454. (g) Zhang, H.; Nomura, K. *Macromolecules* **2006**, *39*, 5266–5274.

(19) Foster, J. P.; Weinhold, F. *J. Am. Chem. Soc.* **1980**, *102*, 7211–7218.

(20) Jezequel, M.; Dufaud, V.; Ruiz-Garcia, M. J.; Carrillo-Hermosilla, F.; Neugebauer, U.; Niccolai, G. P.; Lefebvre, F.; Bayard, F.; Corker, J.; Fiddy, S.; Evans, J.; Broyer, J.-P.; Malinge, J.; Basset, J.-M. *J. Am. Chem. Soc.* **2001**, *123*, 3520–3540.

(21) For example, see: (a) Yasumoto, T.; Yamagata, T.; Mashima, K. *Organometallics* **2005**, *24*, 3375–3377. (b) Buil, M. L.; Esteruelas, M. A.; López, A. M.; Mateo, A. C.; Oñate, E. *Organometallics* **2007**, *26*, 554–565. (c) Wang, C.; Erker, G.; Kehr, G.; Wedeking, K.; Fröhlich, R. *Organometallics* **2005**, *24*, 4760–4773. (d) Qian, Y.; Huang, J.; Bala, M. D.; Lian, B.; Zhang, H.; Zhang, H. *Chem. Rev.* **2003**, *103*, 2633–2690, and references cited therein.

Scheme 1

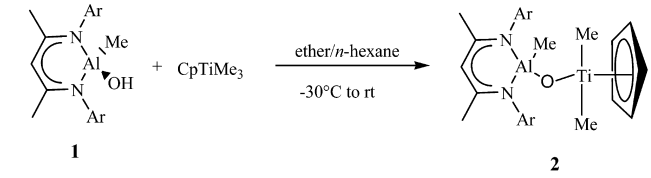

Ar = 2,6-*i*Pr$_2$C$_6$H$_3$

Scheme 2

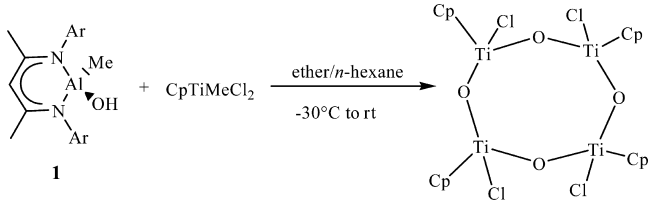

Results and Discussion

In the course of the synthesis of **1**, we followed the improved route by using a strong nucleophilic reagent, N-heterocyclic carbene, as an HCl acceptor for the reaction of LAlMeCl with 1 equiv of water.[22]

Synthesis of LAlMe(μ-O)TiMe$_2$Cp [2; L = CH(N(Ar)-(CMe))$_2$, Ar = 2,6-*i*-Pr$_2$C$_6$H$_3$]. The high oxophilicity of titanium and also the Brönsted acidic character of the proton of the O−H moiety on the aluminum center allowed us to isolate compound **2** under methane elimination at low temperature in high yield. CpTiMe$_3$ was added slowly to the solution of **1** in hexane at −78 °C under vigorous stirring. The mixture was allowed to stir for 10 min before the temperature was slowly raised to 30 °C. It was observed that the transparent solution becomes turbid, indicating the formation of compound **2**. The temperature of the reaction was raised to 0 °C, and stirring was continued for an additional 2 h. Then the temperature was raised to 20 °C under stirring before filtration (Scheme 1).

Efforts were made to isolate the corresponding chloro analogues. However, the reaction of CpTiMeCl$_2$ with **1** yielded the eight-membered Ti$_4$O$_4$ ring (by X-ray structural analysis), indicating that the aluminum and titanium centers exchange the chlorine and oxygen atoms (Scheme 2).[23]

Compound **2** is insoluble in hexane, toluene, and pentane but sparingly soluble in tetrahydrofuran (THF) and ether, whereas it is freely soluble in hot toluene. Complex **2** was characterized by ^{1}H NMR spectroscopy, electron impact (EI) mass spectrometry, elemental analysis, and X-ray structural determination. Compound **2** is a yellow solid that melts at 135 °C. Decomposition was observed at the melting point. Unlike CpTiMe$_3$, compound **2** is thermally stable and not photosensitive. Compound **2** is stable and can be stored for a period of time at room temperature in the absence of air and moisture. The mass spectral data for **2** is in accordance with the assigned structure. Complex **2** does not exhibit a molecular ion. The base peak at *m*/*z* 588 corresponds to [M − 2Me]$^+$. The next most intense peak for compound **2** is observed at *m*/*z* 202, which can be assigned to [Dipp-NCMe]$^+$.[24] The ^{1}H NMR spectrum of **2** exhibits two resonances (δ −0.84 and −0.32 ppm) of 1:2 relative intensities, which can be attributed to the methyl protons of the AlMe and TiMe$_2$ groups, respectively. The characteristic Cp protons for **2** resonate as singlet (δ 5.5 ppm). In addition, a set of resonances assignable to the isopropyl and methyl protons associated with the β-diketiminate ligand is found in the range between δ 1.76 and 1.01 ppm, and the absence of the OH proton resonance features complex **2**. The ^{27}Al NMR is silent because of the quadruple moment of aluminum.

Scheme 3

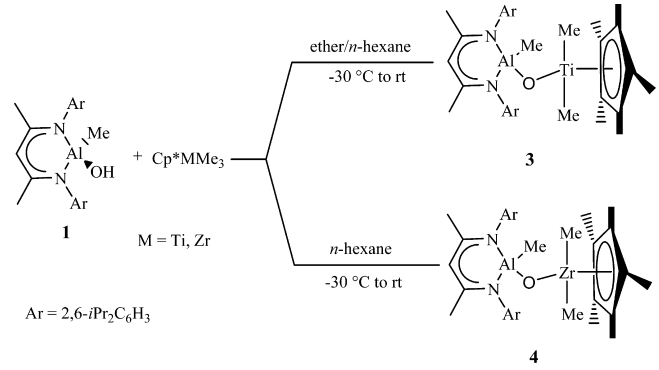

Ar = 2,6-*i*Pr$_2$C$_6$H$_3$

Synthesis of Compounds 3 and 4. The higher stability of Cp*MMe$_3$ (M = Ti, Zr) compared to that of CpTiMe$_3$ allowed its reaction with **1** at room temperature to form the oxygen-bridged heterobimetallic compound LMeAl(μ-O)MMe$_2$Cp* [M = Ti (**3**), Zr (**4**)]. The solution of Cp*MMe$_3$ (M = Ti, Zr) in ether was added drop by drop to the stirred etheral solution of **1** at −30 °C using a cannula. The solution was allowed to stir for 10 min and warmed to room temperature. After stirring for 4 h, the precipitate was filtered off and washed with *n*-hexane before drying under vacuum (Scheme 3).

Compounds **3** and **4** are insoluble in hexane, toluene, and pentane but sparingly soluble in THF and ether, whereas they are freely soluble in hot toluene. Complex **3** was characterized by ^{1}H NMR spectroscopy, EI mass spectrometry, elemental analysis, and X-ray structural analysis, while compound **4** was characterized by ^{1}H NMR spectroscopy, elemental analysis, and X-ray structural analysis. Compound **3** is a yellow crystalline solid that melts at 235 °C, while **4** is a colorless crystalline solid that melts at 181 °C. Decomposition was observed at the melting points of **3** and **4**. Unlike Cp*MMe$_3$ (M = Ti, Zr), complexes **3** and **4** are thermally stable for a long period of time at room temperature in the absence of air and moisture. The mass spectral data for **3** is in accordance with the assigned structure. Compound **3** does not exhibit a molecular ion but shows the base peak at *m*/*z* 658 corresponding to [M − 2Me]$^+$. The next most intense peak was observed at *m*/*z* 202, which can be assigned

(22) Jancik, V.; Pineda, L. W.; Pinkas, J.; Roesky, H. W.; Neculai, D.; Neculai, A. M.; Herbst-Irmer, R. *Angew. Chem.* **2004**, *116*, 2194–2197; *Angew. Chem., Int. Ed.* **2004**, *43*, 2142−2145.

(23) Saunders, L; Spirer, L. *Polymer* **1965**, *6*, 635–644.

(24) Prust, J.; Most, K.; Müller, I.; Alexopoulos, E.; Stasch, A.; Usón, I.; Roesky, H. W. *Z. Anorg. Allg. Chem.* **2001**, *627*, 2032–2037.

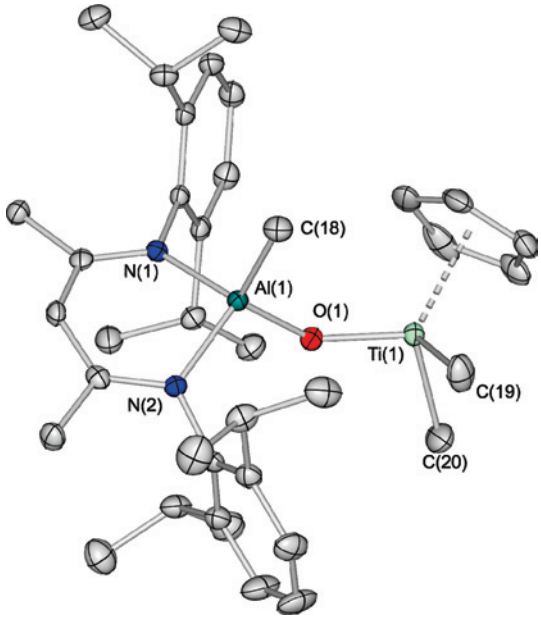

Figure 1. Molecular structure of **2**. Thermal ellipsoids are set at the 50% probability level. H atoms are omitted for clarity.

to $[DippNCMe]^+$.[24] The ^1H NMR spectrum of **3** exhibits two resonances (δ −0.22 and −0.11 ppm) of 1:2 intensities, which can be attributed to the methyl protons of AlMe and $TiMe_2$, respectively, whereas the respective protons of AlMe and $ZrMe_2$ in compound **4** resonate in 1:2 relative intensities (δ −0.23 and −0.32 ppm). The characteristic Cp* protons for **3** and **4** appear as singlets (δ 1.67 and 1.85 ppm). In addition, a set of resonances assignable to the isopropyl and methyl protons associated with the β-diketiminate ligand are found in the range between δ 1.9 and 1.0 ppm, and the absence of the OH proton resonance features both **3** and **4**. The ^{27}Al NMR is silent because of the quadruple moment of aluminum.

Molecular Structure Description of Complexes 2−4. The yellow single crystals of **2** and **3** and the colorless single crystals of **4** were obtained from cooling of their hot toluene solutions and were unambiguously analyzed by X-ray diffraction studies (Figures 1–3). The important bond parameters for compounds **2**−**4** are listed in Table 1.

Compounds **3** and **4** crystallize in the monoclinic space group $P2_1/n$, while complex **2** crystallizes in the triclinic space group $P\bar{1}$. All of the three compounds show the aluminum atom bonded through an oxygen atom to titanium (**2** and **3**) and zirconium (**4**), respectively, and contain a bent Al(μ-O)M (M = Ti, Zr) core. The aluminum atom exhibits a highly distorted tetrahedral geometry with two nitrogen atoms of the β-diketiminato ligand, a methyl group, and one μ-O unit. The titanium (in **2** and **3**) and zirconium (in **4**) exhibit tetrahedral geometry, and their coordination spheres are completed by one Cp′ (Cp′ = Cp in the case of **2** and Cp* in the case of **3** and **4**) ligand, two methyl groups around each metal atom, and one μ-O unit. The methyl groups on aluminum and titanium in **2** and **3** and aluminum and zirconium in **4** are bent out of the Al(μ-O)M (M = Ti, Zr) plane in a trans configuration.

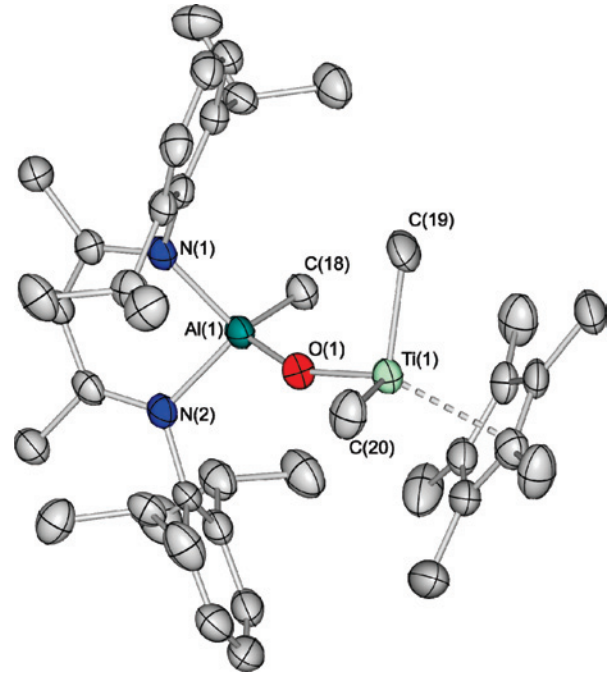

Figure 2. Molecular structure of **3**. Thermal ellipsoids are set at 50% probability level. H atoms are omitted for clarity.

The Al(μ-O) bond lengths in **2** [1.743(1) Å], **3** [1.736(2) Å], and **4** [1.732(2) Å] are similar to each other but slightly longer than those for the bis(cyclopentadienyl) analogues LMeAl(μ-O)MMeCp$_2$ (M = Ti,[11] Zr,[10] Hf[11]) (average 1.71 Å) and significantly longer than those found in compounds $[\{(Me_3Si)_2HC\}_2Al]_2(\mu\text{-}O)$ [1.69(4) Å] and $[HC\{(CMe)(NMe)\}_2AlCl]_2(\mu\text{-}O)$ [1.68(6) Å]. The Al(μ-O)Ti angle [142.2(1)°] in **2** is significantly narrower than the corresponding Al(μ-O)M (M = Ti, Zr) bond angles in **3** [154.0(1)°], **4** [155.37(10)°], and LMeAl(μ-O)MMeCp$_2$ (M = Ti,[11] Zr,[10] Hf[11]) (average 158.3°) complexes. Furthermore, the Al(μ-O)M (M = Ti, Zr) angles in **2**−**4** are considerably less opened than those of homobimetallic M(μ-O)M (M = Zr, Hf) in $(Cp_2ZrMe)_2(\mu\text{-}O)$ [174.1(3)°] and $(Cp_2HfMe)_2(\mu\text{-}O)$ [173.9(3)°]. The Al−Me bond lengths in compounds **2** [1.957(2) Å], **3** [1.956(3) Å], and **4** [1.958(2) Å] are comparable to each other and are similar to those of **1** and LMeAl(μ-O)MMeCp$_2$ [L = CH((CMe)(NAr))$_2$, Ar = 2,6-*i*-Pr$_2$C$_6$H$_3$, M = Ti,[11] Zr,[10] Hf[11]] (average 1.96 Å). Selected bond parameters are listed in Table 2.

The Ti(1)−O(1) bond distance in compound **2** [1.764(1) Å] is slightly shorter than the Ti−O bond lengths in compound **3** [1.778(2) Å] and LMeAl(μ-O)TiMeCp$_2$ [1.808(3) Å][11] but significantly shorter when compared to those in $[Cp_2Ti(CF_3C{=}C(H)CF_3)]_2O$ [average Ti−O 1.86(6)Å] and the alkoxide-bridged clusters $(Ti_4Zr_2O_4(OBu)_n(OMc)_{10}$ [OMc = methacrylate, n = 2, 4, 6; average Ti−O 2.04(5) Å] and $Ti_2(O\text{-}i\text{-}Pr)_2[(O\text{-}2,4\text{-}Me_2C_6H_2\text{-}6\text{-}CH_2)_2(\mu\text{-}OCH_2CH_2)N]_2$ (average Ti−O 1.90 Å). The Ti–Me bond lengths in **2** [2.104(2) and 2.112(2) Å] and **3** [2.111(3) and 2.116(3) Å] are comparable to each other and are slightly shorter when compared to those (average 2.18) in Cp_2TiMe_2. The Ti−XB1A (XB1A = centroid of the Cp ring) distances in **2** (2.084 Å) and **3** (2.082 Å) are identical and are similar to those in dimethyltitanocene (average Ti−XB1A 2.08 Å).

Table 1. Crystal Data and Structure Refinement for Compounds **2**−**4**

	2	**3**	**4**
empirical formula	$C_{37}H_{55}AlN_2OTi$	$C_{42}H_{65}AlN_2OTi$	$C_{42}H_{65}AlN_2OZr$
fw	618.72	688.84	732.16
color	yellow	yellow	colorless
cryst syst	triclinic	monoclinic	monoclinic
space group	$P\bar{1}$	$P2_1/n$	$P2_1/n$
a, Å	9.240(1)	12.033(1)	12.232(2)
b, Å	10.499(1)	19.076(2)	19.009(2)
c, Å	19.982(1)	17.519(1)	17.498(2)
α, deg	91.54(1)	90	90
β, deg	90.02(1)	96.79(1)	97.36(1)
γ, deg	115.26(1)	90	90
V, Å^3	1752.3(3)	3993.1(6)	4035.1(9)
Z	2	4	4
ρ_{calcd}, Mg m^{-3}	1.173	1.146	1.205
σ, mm^{-1}	2.526	2.263	2.675
$F(000)$	668	1496	1568
θ range for data collection, deg	4.43−59.06	3.44−59.00	3.45−59.39
index ranges	$-10 \le h \le 10$ $-11 \le k \le 11$ $-22 \le l \le 22$	$-13 \le h \le 13$ $-20 \le k \le 21$ $-19 \le l \le 19$	$-13 \le h \le 13$ $-21 \le k \le 21$ $-19 \le l \le 19$
no. of reflns collcd	18 109	30 327	35 043
no. of indep reflns (R_{int})	4920 (R_{int} = 0.0313)	5577 (R_{int} = 0.0711)	5798 (R_{int} = 0.0532)
refinement method	full-matrix least squares on F^2	full-matrix least squares on F^2	full-matrix least squares on F^2
GOF	1.080	1.046	1.034
final R indices [$I > 2\sigma(I)$]	R1 = 0.0288, wR2 = 0.0783	R1 = 0.0508, wR2 = 0.1298	R1 = 0.0291, wR2 = 0.736
R indices (all data)[a,b]	R1 = 0.0298, wR2 = 0.0789	R1 = 0.0730, wR2 = 0.1442	R1 = 0.0339, wR2 = 0.0771
largest diff peak/hole (e Å^{-3})	−0.255/+0.281	−0.517/+0.326	−0.408/+0.383

[a] $R1 = \sum|F_o| - |F_c|/\sum|F_o|$. [b] $wR2 = [\sum w(F_o^2 - F_c^2)^2/\sum w(F_o^2)^2]^{0.5}$.

Table 2. Selected Bond Distances (Å) and Angles (deg) for Compounds **2**−**4**[a]

	Compound **2**		
Ti(1)−O(1)	1.764(1)	Al(1)−O(1)	1.743(1)
Ti(1)−C(19)	2.104(2)	Al(1)−N(1)	1.913(1)
Ti(1)−C(20)	2.112(2)	Al(1)−N(2)	1.894(1)
Ti(1)−X1A	2.084	Al(1)−C(18)	1.957(2)
Al(1)−O(1)−Ti(1)	142.2(1)	O(1)−Al(1)−C(18)	113.27(7)
O(1)−Ti(1)−C(19)	105.19(6)	O(1)−Al(1)−N(1)	110.51(6)
O(1)−Ti(1)−C(20)	102.50(7)	O(1)−Al(1)−N(2)	109.46(6)
N(1)−Al(1)−C(18)	111.83(7)	N(2)−Al(1)−C(18)	113.95(7)
C(19)−Ti(1)−C(20)	97.85(8)	N(1)−Al(1)−N(2)	96.65(6)
X1A−Ti(1)−O(1)	121.9	X1A−Ti(1)−C(19)	114.3
X1A−Ti(1)−C(20)	111.9		
	Compound **3**		
Ti(1)−O(1)	1.778(2)	Al(1)−O(1)	1.736(2)
Ti(1)−C(19)	2.111(3)	Al(1)−N(1)	1.916(2)
Ti(1)−C(20)	2.116(3)	Al(1)−N(2)	1.921(2)
Ti(1)−X1A	2.082	Al(1)−C(18)	1.956(3)
Al(1)−O(1)−Ti(1)	154.0(1)	O(1)−Al(1)−C(18)	114.4(1)
O(1)−Ti(1)−C(19)	101.1(11)	O(1)−Al(1)−N(1)	112.6(10)
O(1)−Ti(1)−C(20)	106.4(1)	O(1)−Al(1)−N(2)	111.3(1)
N(1)−Al(1)−C(18)	111.9(1)	N(2)−Al(1)−C(18)	108.9(1)
C(19)−Ti(1)−C(20)	97.0(2)	N(1)−Al(1)−N(2)	96.3(1)
X1A−Ti(1)−O(1)	124.5	X1A−Ti(1)−C(19)	112.5
X1A−Ti(1)−C(20)	111.15		
	Compound **4**		
Zr(1)−O(1)	1.920(2)	Al(1)−O(1)	1.732(2)
Zr(1)−C(19)	2.271(3)	Al(1)−N(1)	1.910(2)
Zr(1)−C(20)	2.249(2)	Al(1)−N(2)	1.921(2)
Zr(1)−X1A	2.231	Al(1)−C(18)	1.958(2)
O(1)−Zr(1)−C(19)	109.08(9)	O(1)−Al(1)−N(1)	111.19(7)
O(1)−Zr(1)−C(20)	102.32(8)	O(1)−Al(1)−N(2)	111.23(7)
C(19)−Zr(1)−C(20)	100.07(11)	N(1)−Al(1)−N(2)	96.36(7)
N(1)−Al(1)−C(18)	112.73(8)	N(2)−Al(1)−C(18)	109.31(9)
Al(1)−O(1)−Zr(1)	155.37(10)	O(1)−Al(1)−C(18)	114.57(10)
X1A−Zr(1)−O(1)	122.2	X1A−Zr(1)−C(19)	109.7
X1A−Zr(1)−C(20)	111.0		

[a] XB1A = centroid of the Cp ring.

The Zr(1)−O(1) bond distance in **4** [1.920(2) Å] is shorter compared to the corresponding bond length in the oxygen-bridged (μ-O) compounds $(Cp_2ZrL)_2(\mu\text{-O})$ [L = Me, SC_6H_5; 1.95(1) and 1.97(5) Å] and $Cp^*_2MeZr(\mu\text{-O})TiMe_2Cp^*$ [Zr−O 2.02(4) Å].[13] The Zr−C bond lengths [2.271(3) and 2.249(2) Å] in **4** are comparable to that in the heterobimetallic compound $Cp^*_2MeZr(\mu\text{-O})TiMe_2Cp^*$ (2.30 Å).[13] The Zr−XB1A distance (2.231 Å) in **4** is comparable to that in dimethylzirconocene (average Zr−XB1A 2.3 Å).[25]

Accounting for the Thermal Stability of Compounds 2−4. The thermal stability of the metallocene catalysts is one of the most important factors for their application in industry.[26] For efficient catalytic processes, the ideal situation is that the catalyst has to be both highly active and thermally stable. The instability of the $Cp'MMe_3$ (Cp′ = Cp or Cp*; M = Ti or Zr)[16] complexes does not allow to use them in the polymerization reactions. The heterobimetallic complexes **2**−**4** exhibit good thermal stability and can be stored for a long period of time in the absence of air or moisture, unlike their precursors, which should be stored only at very low temperature. The heterobimetallic complexes are stable to air and moisture for a short period of time, while their precursors are very sensitive to air and moisture. For example, $CpTiMe_3$[16] is only stable below −30 °C, while compound **2** decomposes at 135 °C.

Ethylene Polymerization Studies of Compounds 2 and 3. In the presence of MAO, compounds **2** and **3** act as catalysts and exhibit high catalytic activity for the polymerization of ethylene. All polymeric materials were isolated as white powders. Table 3 summarizes the polymerization

(25) Hunter, W. E.; Hrncir, D. C.; Bynum, R. V.; Penttila, R. A.; Atwood, J. L. *Organometallics* **1983**, *2*, 750–755.
(26) Jia, L.; Yang, X.; Stern, C. L.; Marks, T. J. *Organometallics* **1997**, *16*, 842–875.

Table 3. Ethylene Polymerization Data for Compounds **2** and **3**[a]

catalyst	MAO/catalyst	t (min)	PE (g)	$A \times 10^5$	M_w	M_w/M_n	T_m (°C)
2	100	30	0.3	0.3			121
2	200	30	0.9	0.9	103 263	2.84	127
2	300	30	1.7	1.6	225 027	4.23	124
2	400	30	3.1	3.0			129
3	100	30	0.8	0.8			119
3	200	30	1.7	1.6	124 265	4.02	127
3	300	30	3.6	3.4	470 431	3.14	130
3	400	30	5.0	4.8			129

[a] Polymerization conditions: **2** and **3** = 21 μmol, 100 mL of toluene at 25 °C, 1 atm of ethylene pressure. Activity (A) = g of PE/mol of catalyst·h.

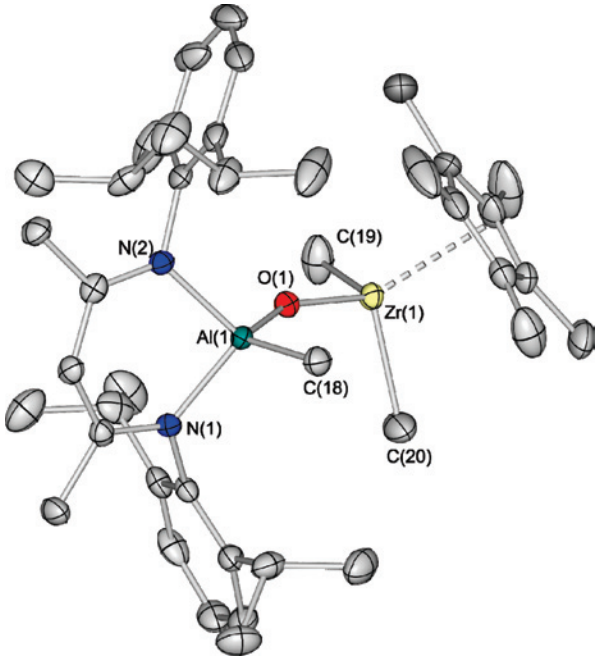

Figure 3. Molecular structure of **4**. Thermal ellipsoids are set at the 50% probability level. H atoms are omitted for clarity.

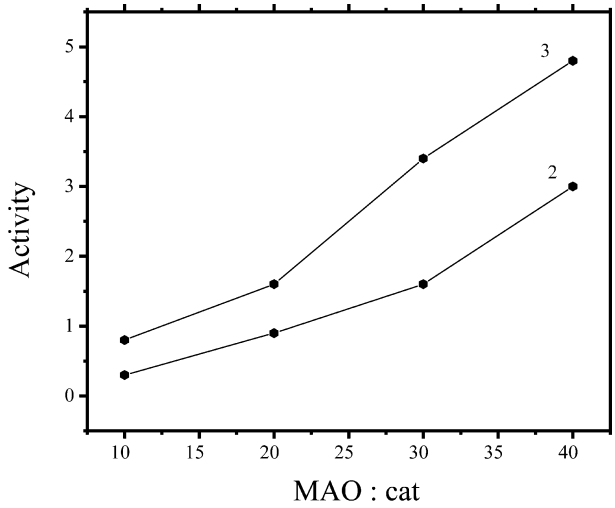

Figure 4. Comparative plot of the activity toward the MAO/catalyst ratio for compounds **2** and **3** in ethylene polymerization.

results of compounds **2** and **3**. Under comparable polymerization conditions, both MAO/**2** and MAO/**3** catalyst systems show lower activity compared to that of MAO/LAlMe(μ-O)M(Me)Cp_2 (M = Ti,[11] Zr[10]). Figure 4 exhibits a plot of activities for different ratios of MAO/**2** and MAO/**3**, revealing a gradual increase in the activity with the MAO/catalyst ratios. In general, the activities of the bisCp complexes were found to be the highest, about 10 orders of magnitude more than those of the monoCp′ (Cp′ = Cp or Cp*) analogues. The same trend was previously reported in the literature.[20] The data presented in Table 3 clearly demonstrate that both compounds **2** and **3** act as active catalysts even at low MAO/catalyst ratios; a similar result was previously observed for the corresponding LAlMe(μ-O)M(Me)Cp_2 (M = Ti,[11] Zr[10]) complexes. The plot of activities for compounds **2** and **3** indicates that compound **3** is more active than compound **2** under comparable conditions. This may be due to the formation of a more stable cation in **3**, which has a bulky and more electron-donating Cp* ligand in its coordination sphere compared to **2**, which has a less steric and less electron-donating Cp ligand. Unfortunately, compound **4** could not be isolated in a pure form; it always crystallizes with impurities.

Table 4. Styrene Polymerization Data for Compounds **2** and **3**[a]

catalyst	MAO/catalyst	t (min)	PS (g)	$A \times 10^4$	T_g (°C)
2	400	60	0.3	1.4	87
2	800	60	0.8	3.8	93
2	1200	60	1.1	5.2	87
2	1600	60	1.7	8.1	81
3	400	60	0.4	1.9	91
3	800	60	1.0	4.8	89
3	1200	60	1.4	6.7	97
3	1600	60	2.5	12.0	88

[a] Polymerization conditions: **2** and **3** = 21 μmol, 100 mL of toluene at 25 °C, 10 mL of styrene under argon. Activity (A) = g of PS/mol of catalyst·h.

PE Properties. Melting points (T_m) for the polymers are in the range of 119−130 °C, and ^{13}C NMR spectra exhibit a single resonance at around 30 ppm, which can be attributed to the backbone carbon of linear PE. The gel permeation chromatography (GPC) for measured PE samples exhibits monomodal property for measured PE samples. The polydispersities show narrow distribution ranging from 2.8 to 4.2, which corresponds to single-site catalysts (Table 3).[1]

Styrene Polymerization Studies for Compounds 2 and 3. The catalytic properties of complexes **2** and **3** for the polymerization of styrene were preliminarily investigated. These complexes show living catalyst activity at ambient temperature in toluene when activated with MAO. All polymeric materials were isolated as white powders, and Table 4 summarizes the activity values of catalysts **2** and **3**. Figure 5 exhibits a plot for activity versus MAO/catalyst ratio.

Properties of PS Produced by 2 and 3. The differential scanning calorimetry (DSC) measurements of the polymers show that the characteristic glass transition temperatures (T_g) are in the range from 81 to 97 °C, which is within the typical T_g range for the atactic polymers. As expected, compound **3** shows more activity compared to that of compound **2** because of the formation of a more stable cation intermediate in **3** when compared to **2**.

Ethylene and Styrene Copolymerization Studies for Compounds 2 and 3. Preliminary investigations of ethylene and styrene copolymerization reactions were carried out. The

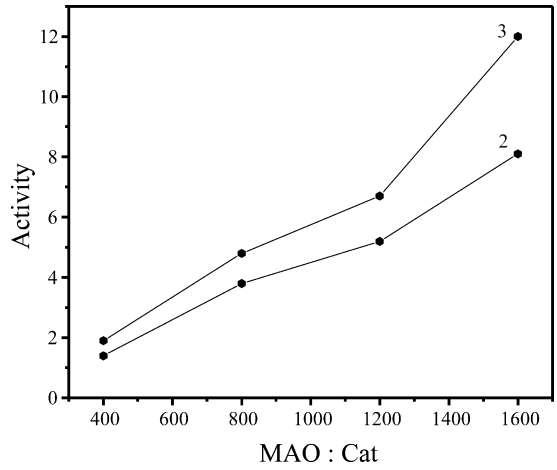

Figure 5. Comparative plot of the activity toward the MAO/catalyst ratio for compounds **2** and **3** in styrene polymerization.

Table 5. Ethylene and Styrene Copolymerization Data for Compounds **2** and **3**[a]

catalyst	MAO/ catalyst	t (min)	PE (g)	$A \times 10^5$	M_w	M_w/M_n	T_m (°C)
2	200	60	0.82	0.39			117
2	400	60	1.70	0.81			116
3	200	60	1.31	0.62			119
3	400	60	2.00	0.95	422018	7.17	120

[a] Polymerization conditions: **2** and **3** = 21 μmol, 100 mL of toluene at 25 °C, at 1 atm of ethylene pressure, 10 mL of styrene. Activity (A) = g of PE/mol of catalyst·h.

MAO-activated complexes **2** and **3** exhibit moderate catalytic activity and produce polymer products. These polymer products were characterized in order to observe the incorporation of styrene into ethylene, which can produce polymers of interesting microstructure. The DSC measurements of the polymers show that the melting point temperatures (T_m) are in the range from 116 to 119 °C. The ^{13}C NMR spectra exhibits only one peak (~30.0 ppm) corresponding to the backbone carbon. These data indicate that the polymer produced by **2** and **3** is PE. The styrene incorporation is negligible (even we can say there is no styrene incorporation) because we did not observe any other resonances in the ^{13}C NMR spectra. The copolymerization results in homopolymerization of ethylene (Table 5).

Experimental Section

General Comments. All experimental manipulations were carried out under an atmosphere of dry argon using standard Schlenk techniques. The samples for spectral measurements were prepared in a glovebox. The solvents were purified according to conventional procedures and were freshly distilled prior to use. $CpMCl_3$ and Cp^*MCl_3 (M = Ti, Zr) were purchased from Aldrich, and methyl derivatives were prepared by procedures that were published elsewhere.[16] NMR spectra were recorded on a Bruker Avance 300 instrument, and the chemical shifts are reported with reference to tetramethylsilane (TMS). ^{13}C NMR assays of the polymer microstructure were conducted in 1,1,2,2-tetrachloroethane-d_2 at 90 °C. Resonances were assigned according to the literature for PE.[3] Mass spectra were obtained on a Finnigan MAT 8230 spectrometer by the EI technique. Melting points were measured in sealed capillaries on a Büchi B 540 instrument. Elemental analyses were performed at the Analytical Laboratory of the Institute of Inorganic Chemistry at Göttingen, Germany.

Synthesis of LAlMe(μ-O)TiMe$_2$Cp (2). A solution of freshly prepared $CpTiMe_3$ (0.21 g, 1.01 mmol) in toluene (20 mL) was added via a cannula to a solution of **1** (0.48 g, 1.01 mmol) in toluene (20 mL) at −30 °C. The mixture was stirred at −30 °C for 1 h, then the temperature was slowly raised to 0 °C, and the stirring was continued. After 3 h, the solution was allowed to attain room temperature and stirred for 12 h. (**Caution!** *Care must be taken because methyl derivatives of titanium are photosensitive.*) The yellow precipitate formed was filtered off, washed with *n*-hexane, and dried in vacuum. Yield: 0.41 g (61%). Mp: 135 °C (dec). ^1H NMR (500.13 MHz, C_6D_6, 25 °C, TMS): δ 7.1−7.2 (m, 6H, *m*- and *p*-Ar*H*), 5.50 (s, 5H, C_5H_5), 5.14 (s, 1H, γ-C*H*), 3.38 (sept, 2H, $^3J_{H-H}$ = 6.8 Hz, C*H*(CH$_3$)$_2$), 3.11 (sept, 2H, $^3J_{H-H}$ = 6.8 Hz, C*H*(CH$_3$)$_2$), 1.73 (s, 6H, CH_3), 1.25 (d, 12H, $^3J_{H-H}$ = 6.8 Hz, CH(CH_3)$_2$), 1.15 (d, 12H, $^3J_{H-H}$ = 6.80 Hz, CH(CH_3)$_2$), −0.32 (s, 3H, TiCH_3)), −0.84 (s, 3H, AlCH_3)) ppm. MS (EI) *m*/*z* (%): 588 (100) [M$^+$ − 2Me], 202 (26) [DippNCMe]$^+$. Anal. Calcd for $C_{37}H_{55}AlN_2OTi$ (618.69): C, 71.83; H, 8.96; N, 4.53. Found: C, 70.01; H, 8.93; N, 5.37.

Synthesis of LAlMe(μ-O)TiMe$_2$Cp* (3). Freshly sublimed Cp^*TiMe_3 (0.34 g, 1 mmol) dissolved in ether (20 mL) was transferred using a cannula to a flask charged with **1** (0.48 g, 1 mmol) in diethyl ether (30 mL) at −30 °C. The reaction mixture was slowly warmed to ambient temperature and stirred for 12 h. The yellow precipitate was filtered, washed with *n*-hexane, and dried in vacuum. Yield: 0.54 g (67.4%). Mp: 235 °C (dec). ^1H NMR (500.13 MHz, C_6D_6, 25 °C, TMS) δ 7.13−7.24 (m, 6H, *m*- and *p*-Ar*H*), 4.90 (s, 1H, γ-C*H*), 3.69 (sept, 4H, $^3J_{H-H}$ = 6.8 Hz, C*H*(CH$_3$)$_2$), 3.34 (sept, 4H, $^3J_{H-H}$ = 6.8 Hz, C*H*(CH$_3$)$_2$), 1.67 (s, 15H, C$_5$(CH_3)$_5$), 1.64 (s, 6H, CH_3), 1.50 (d, 6H, $^3J_{H-H}$ = 6.8 Hz, CH(CH_3)$_2$), 1.44 (d, 6H, $^3J_{H-H}$ = 6.8 Hz, CH(CH_3)$_2$), 1.23 (d, 6H, $^3J_{H-H}$ = 6.8 Hz, CH(CH_3)$_2$), 1.22 (d, 6H, $^3J_{H-H}$ = 6.8 Hz, CH(CH_3)$_2$), −0.11 (s, 6H, TiCH_3)$_2$), −0.22 (s, 6H, AlCH_3) ppm. MS (EI) *m*/*z* (%): 658 (100) [M$^+$ − 2Me], 770 (8) [M$^+$ − 2Me], 202 (26) [DippNCMe]$^+$. Anal. Calcd for $C_{42}H_{65}AlN_2OTi$ (688.83): C, 73.23; H, 9.51; N, 4.07. Found: C, 72.88; H, 9.43; N, 3.98.

Synthesis of LAlMe(μ-O)ZrMe$_2$Cp* (4). A solution of freshly prepared Cp^*ZrMe_3 (0.21 g, 1.01mmol) in toluene (20 mL) was added via a cannula to a solution of **1** (0.48 g, 1.01 mmol) in toluene (20 mL) at −30 °C. The mixture was stirred at −30 °C for 3 h and then slowly raised to 0 °C, and the stirring was continued for 12 h. The white precipitate formed was filtered off, washed with *n*-hexane, and dried in vacuum. Yield: 0.57 g (73%). Mp: 181 °C (dec). ^1H NMR (500.13 MHz, C_6D_6, 25 °C, TMS): δ 7.13−7.24 (m, 6H, *m*- and *p*-Ar*H*), 4.92 (s, 1H, γ-C*H*), 3.65 (sept, 4H, $^3J_{H-H}$ = 6.8 Hz, C*H*(CH$_3$)$_2$), 3.36 (sept, 4H, $^3J_{H-H}$ = 6.8 Hz, C*H*(CH$_3$)$_2$), 1.85 (s, 15H, C$_5$(CH_3)$_5$), 1.78 (s, 6H, CH_3), 1.63 (d, 6H, $^3J_{H-H}$ = 6.8 Hz, CH(CH_3)$_2$), 1.60 (d, 6H, $^3J_{H-H}$ = 6.8 Hz, CH(CH_3)$_2$), 1.30 (d, 6H, $^3J_{H-H}$ = 6.8 Hz, CH(CH_3)$_2$), 1.22 (d, 6H, $^3J_{H-H}$ = 6.8 Hz, CH(CH_3)$_2$), −0.23 (s, 3H, AlCH_3), −0.32 (s, 6H, ZrCH_3)$_2$) ppm. Anal. Calcd for $C_{42}H_{65}AlN_2OZr$ (732.18): C, 68.90; H, 8.95; N, 3.83. Found: C, 68.28; H, 8.93; N, 3.58.

X-ray Structure Determination of 2−4. Data for the structures **2**−**4** were collected on a Bruker three-circle diffractometer equipped with a SMART 6000 CCD detector. Intensity measurements were performed on a rapidly cooled crystal. The structures were solved by direct methods (*SHELXS-97*)[27] and refined with all data by full-matrix least squares on F^2.[28] The hydrogen atoms on C−H bonds were placed in idealized positions and refined isotropically with a

(27) Sheldrick, G. M. *Acta Crystallogr.* **1990**, *A46*, 467–473.
(28) Sheldrick, G. M. *SHELXS-97 and SHELXL-97. Program for Crystal Structure Refinement*; Göttingen University: Göttingen, Germany, 1997.

riding model, whereas the non-hydrogen atoms were refined anisotropically. They were refined with distance restraints and restraints for the anisotropic displacement parameters. Crystal data and selected bond lengths and angles are shown in Tables 1 and 2.

Ethylene Polymerization Experiments. Ethylene polymerizations were carried out on a vacuum line (10^{-5} Torr) in an autoclave (Büchi). In a typical experiment, the catalyst (see Table 3) was taken and an appropriate amount of MAO (1.6 M, Aldrich) was added and stirred for 20 min for the activation. After stirring, the resulting mixture was placed into the autoclave by using a gastight syringe, which was previously saturated with 100 mL of toluene under an ethylene atmosphere (1 atm). After stirring for an appropriate time, the reaction was quenched using methanol and the white PE formed was collected by filtration and dried.

Styrene Polymerization Experiments. Styrene polymerizations were carried out on a vacuum line (10^{-5} Torr) in an autoclave (Buchi). In a typical experiment, the catalyst (see Table 4) was taken and an appropriate amount of MAO (1.6 M, Aldrich) was added and stirred for 20 min for the activation. After stirring, the resulting mixture was placed into the autoclave by using a gastight syringe, which was previously saturated with argon, 100 mL of toluene, and 10 mL of styrene. After stirring for an appropriate time, the reaction was quenched using methanol and the white PS formed was collected by filtration and dried.

Ethylene and Styrene Copolymerization Experiments. Copolymerization of ethylene and styrene was carried out on a vacuum line (10^{-5} Torr) in an autoclave (Büchi). In a typical experiment, the catalyst (see Table 5) was taken and an appropriate amount of MAO (1.6 M, Aldrich) was added and stirred for 20 min for the activation. After stirring, the resulting mixture was placed into the autoclave by using a gastight syringe. The autoclave was previously saturated with purified ethylene (1 atm), 100 mL of toluene, and 10 mL of styrene. After stirring for an appropriate time, the reaction was quenched using methanol and the white PE formed was collected by filtration and dried.

DSC. The polymer melting range was measured on a TA Instrument 2920 (modulated differential scanning calorimeter), which was calibrated against indium metal (ca. 4 mg samples were used at 10 °C/min).

GPC. GPC was carried out at Basell R&D Polymer Physics and Characterization, Industriepark, Hoechst, Frankfurt, Germany. 1,2,4-Trichlorobenzene was used as the solvent. The columns were calibrated with narrow molar mass distribution standards of PS.

Acknowledgment. This work was supported by the Göttinger Akademie der Wissenschaften, Deutsche Forschungsgemeinschaft, and the Fonds der Chemischen Industrie. The authors thank Dr. Volker Dolle for his kind help in analyzing polymer samples by GPC.

Supporting Information Available: X-ray crystallographic data of **2**−**4** in CIF format. This material is available free of charge via the Internet at http://pubs.acs.org.

IC800198E